

Spin-polarized tunneling through potential barriers at ferromagnetic metal/semiconductor Schottky contacts

D. L. Smith

Los Alamos National Laboratory, Los Alamos, New Mexico 87545, USA

P. P. Ruden

University of Minnesota, Minneapolis, Minnesota 55455, USA

(Received 5 February 2008; revised manuscript received 29 July 2008; published 10 September 2008)

A model for electron tunneling through a space-charge induced potential barrier at a semiconductor/ferromagnetic metal Schottky contact is developed and applied to the exploration of the bias dependence of the spin-polarized tunneling current. It is found that significant bias dependence of the spin polarization of the current can result from changes in the shape of the potential barrier due to the applied voltage. Specifically, we show that the dependence of the transmission coefficient on the shape of the barrier potential can lead to a nonmonotonic bias dependence of the spin current and may result in a reversal of the sign of the spin-current polarization at small voltages. Numerical results are presented for GaAs/Fe Schottky contacts.

DOI: [10.1103/PhysRevB.78.125202](https://doi.org/10.1103/PhysRevB.78.125202)

PACS number(s): 72.25.Mk

I. INTRODUCTION

Ferromagnetic metal contacts to semiconductors are of current interest due to their potential use in spintronic devices.¹ Exploiting the electron spin in information processing semiconductor devices requires the ability to inject spin-polarized charge carriers, to control their spin while they transit the semiconductor, and to extract them in a way that is sensitive to their spin. The first and last requirements are, in principle, met by ferromagnetic metal contacts to semiconductors. It has been shown that injecting charge carriers with significant spin polarization from a ferromagnetic metal into a (nonmagnetic) semiconductor is possible through an injection process that is itself spin dependent.² Tunneling through a potential barrier can provide such a mechanism³ and spin-polarized injection has been demonstrated to be effective in Fe/GaAs (Ref. 4) and Fe/AlGaAs (Ref. 5) Schottky contacts and Fe/Al₂O₃/Si contacts.⁶ The Fe/GaAs material system, in particular, is being explored extensively because high-quality epitaxial interfaces can be prepared. Somewhat unexpectedly, recent work has shown that the spin polarization of the injected charge carriers varies significantly with the bias voltage applied and that it may even change sign.⁷⁻⁹ Valenzuela *et al.*⁷ explored the dynamic tunnel resistance of Fe/Al₂O₃/Al structures and Crooker *et al.*⁸ reported experiments on Fe/GaAs Schottky contacts that showed equal sign of the spin current for forward and reverse biases, implying a change in sign of the relative current polarization between the two voltages applied. More detailed subsequent investigations⁹ observed the change in sign in the current polarization at -0.1 V for two Fe/GaAs contact samples and at $+0.01$ V for another. Additional relevant experimental work was reported in Ref. 10.

A possible explanation for the bias dependence of the spin polarization, based on details of the electronic structure of the Fe/GaAs interface, has been proposed by Chantis *et al.*¹¹ That work focuses on the transfer of electrons through the Fe/GaAs interface and does not address the bias dependence of the tunneling probability through the depletion region,

which is the subject of the model presented in this work.

Spin extraction through Fe/GaAs Schottky contacts has been examined recently by Dery and Sham.¹² These authors pointed out that the highly doped region near the metal/semiconductor interface, which is used to fabricate spin injection structures, may give rise to bound states in the semiconductor near the interface, and that these bound states can affect the spin polarization of the electron transfer between the semiconductor and the metal leading to a bias dependence of the spin polarization.

In the present work we show that the voltage dependence of the shape of the potential barrier through which the electrons tunnel may lead to a strong bias voltage dependence of their spin polarization. To ensure wide applicability of the model, few assumptions regarding details of the electronic structure of the metal and the semiconductor/metal interface are made. It is found that, even in absence of pronounced features in the electronic structure of the ferromagnetic contact or of bound states in the semiconductor near the interface, the sign of the injected carrier polarization may change with the applied voltage.¹³ We describe the model in Sec. II and present a simple analytical approximation followed by numerical results for Fe/GaAs parameters in Sec. III. Conclusions are drawn in Sec. IV. The appendix presents a brief outline of an alternative numerical treatment.

II. MODEL DESCRIPTION

The model developed in this work represents contacts of the general type studied experimentally, i.e., ferromagnetic contacts (Fe in Refs. 8 and 9) that form well-defined Schottky contacts on an n -type semiconductor (GaAs in Refs. 8 and 9). To enable significant tunneling of electrons through the space-charge potential barrier the semiconductor is assumed to be heavily doped near the contact interface. The domain of interest for the model is divided into three spatial regions as shown in Fig. 1. A voltage applied to the (n -doped) semiconductor/metal contact drops across a layer bounded by $z=0$ (in the semiconductor) and $z=d$ (at the

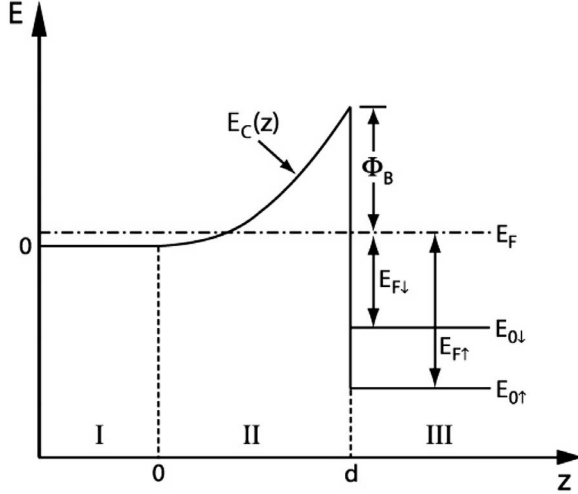


FIG. 1. Schematic band diagram of the semiconductor/ferromagnetic metal contact in equilibrium. The region of the semiconductor displayed is assumed to be degenerately doped (n type). The energies $E_{0\uparrow}$ and $E_{0\downarrow}$ denote the lower edges of the majority-spin and minority-spin bands in the ferromagnetic metal.

semiconductor/metal interface). Wave functions that are solutions to the electronic structure problem in regions I and II need to be matched at $z=0$, and wave functions for regions II and III need to satisfy matching conditions at $z=d$.

The spin polarization of the tunneling current between regions I and III can depend on the voltage applied because (a) the electronic states in regions I and III that participate in the tunneling process shift relative to each other with bias and different semiconductor and metal states participate in tunneling at different bias voltages and (b) the barrier potential changes shape with applied voltage causing the spin dependence of the transmission coefficients at a fixed energy to vary. In Ref. 12 the effect of bound states that can form in the semiconductor near the interface because of the doping profile was studied. The relative importance of the contribution to tunneling from these bound states depends on bias and can change the spin polarization of the tunneling current. In Ref. 11 the influence of an interface resonance state for minority spins near the Fermi energy at the Fe/GaAs interface was studied and found to lead to a voltage dependence of the spin polarization of the tunneling current. The model presented in this work focuses specifically on the effect of the change in the shape of the tunnel barrier on the spin polarization of the tunneling current.

The relevant electronic states of the (nonmagnetic) semiconductor are assumed to be described by effective-mass theory with a conduction-band minimum at the Γ point. The wave functions in region I consist of incident and reflected Bloch states in the bulk semiconductor ($z < 0$). They are written as

$$\psi_I(\vec{r}) = (1/\sqrt{N})e^{i\vec{k}_{\parallel}\vec{r}_{\parallel}}[e^{ik_{z,s}^0 z} + R e^{-ik_{z,s}^0 z}]u_0(\vec{r}). \quad (1)$$

Here, u_0 is the cell-periodic part of the Bloch function at the Γ point and the normalization volume consists of N unit cells (of volume Ω_0).

In region II, the potential barrier layer, the effective-mass Schrödinger equation yields two linearly independent (real) solutions for the envelope function, $\Phi_1(z)$ and $\Phi_2(z)$. We choose the combination of the solution functions that satisfy $\Phi_1(0)=1$, $\frac{d\Phi_1}{dz}|_0=0$ and $\Phi_2(0)=0$, $\frac{d\Phi_2}{dz}|_0=\frac{1}{\lambda}$. ($1/\lambda$ is the Wronskian of Φ_1 and Φ_2 and is independent of z .) Matching the wave function and its derivative at $z=0$, we obtain for region II

$$\psi_{II}(\vec{r}) = (1/\sqrt{N})e^{i\vec{k}_{\parallel}\vec{r}_{\parallel}}[(1+R)\Phi_1(z) + ik_{z,s}^0\lambda(1-R)\Phi_2(z)]u_0(\vec{r}), \quad (2)$$

where the coefficient R is determined by matching conditions at the interface between regions II and III. It is convenient to work with the Fourier transforms of the envelope functions defined by $\hat{\Phi}_i(k_{z,s}) = (1/L)\int_0^L dz \Phi_i(z)\exp(-ik_{z,s}z)$, where L denotes the normalization length. Separating forward and backward propagating parts, the total wave function in region II becomes

$$\begin{aligned} \Psi_{II}(\vec{r}) = (1/\sqrt{N})e^{i\vec{k}_{\parallel}\vec{r}_{\parallel}} \sum_{k_{z,s} \geq 0} \{ & [(1+R)\hat{\Phi}_1(k_{z,s}) \\ & + ik_{z,s}^0\lambda(1-R)\hat{\Phi}_2(k_{z,s})]e^{ik_{z,s}z} + [(1+R)\hat{\Phi}_1(-k_{z,s}) \\ & + ik_{z,s}^0\lambda(1-R)\hat{\Phi}_2(-k_{z,s})]e^{-ik_{z,s}z}\} u_0(\vec{r}). \end{aligned} \quad (3)$$

Here the sum includes only non-negative $k_{z,s}$. The wave function in region II is now a sum of terms of form $\alpha\psi_s^+ + \beta\psi_s^-$, where ψ_s^+ and ψ_s^- are effective-mass states of wave vector $(\vec{k}_{\parallel}, k_{z,s})$ and $(\vec{k}_{\parallel} - k_{z,s})$ that propagate toward and away from the metal/semiconductor interface, respectively.

The boundary conditions at the metal/semiconductor interface may be written as $J_z|\psi_{II}\rangle = J_z|\psi_{III}\rangle$, where J_z is the z component of the current-density operator at $z=d$ and ψ_{III} is the component of the wave function in region III.^{14,15} We consider the case of a (specular) interface that does not induce scattering between states of different \vec{k}_{\parallel} . Hence, ψ_{III} is a linear combination of metal Bloch states with wave vectors $(\vec{k}_{\parallel}, k_{z,m})$ and $(\vec{k}_{\parallel} - k_{z,m})$ near the Fermi level, $\psi_{III} = \gamma\psi_m^+ + \delta\psi_m^-$. The interface matching conditions may be written as

$$\begin{aligned} \alpha\langle\psi_s^+|J_z|\psi_s^+\rangle_{av} + \beta\langle\psi_s^+|J_z|\psi_s^-\rangle_{av} &= \gamma\langle\psi_s^+|J_z|\psi_m^+\rangle_{av} \\ &+ \delta\langle\psi_s^+|J_z|\psi_m^-\rangle_{av}, \\ \alpha\langle\psi_s^-|J_z|\psi_s^+\rangle_{av} + \beta\langle\psi_s^-|J_z|\psi_s^-\rangle_{av} &= \gamma\langle\psi_s^-|J_z|\psi_m^+\rangle_{av} \\ &+ \delta\langle\psi_s^-|J_z|\psi_m^-\rangle_{av}, \end{aligned} \quad (4)$$

where the coefficients α and β have the form given in Eq. (3).

The matrix elements are integrated over a unit cell at the interface. The matrix elements that involve wave functions in one material only (here the semiconductor) are readily evaluated as $\langle\psi_s^{\pm-}|J_z|\psi_s^{\pm-}\rangle_{av} = \pm(\hbar k_z/m^*)/(N\Omega_0)$ and $\langle\psi_s^{\pm-}|J_z|\psi_s^{\pm+}\rangle_{av} = 0$ if the system has a C_2 symmetry axis parallel to the z direction, as is the case for (100) GaAs/Fe, in addition to time-reversal symmetry. Furthermore, the same symmetry considerations yield for the matrix elements that connect regions II and III,

$$\begin{aligned}\langle \psi_s^+ | J_z | \psi_m^+ \rangle_{av} &= \frac{1}{N\Omega_0} e^{i(k_{z,m} - k_{z,s})d} [I(\vec{k}_s^+, \vec{k}_m^+) - I(\vec{k}_m^-, \vec{k}_s^-)] \\ &= -\langle \psi_s^- | J_z | \psi_m^- \rangle_{av}^*, \\ \langle \psi_s^+ | J_z | \psi_m^- \rangle_{av} &= \frac{1}{N\Omega_0} e^{i(k_{z,s} + k_{z,m})d} [I(\vec{k}_s^+, \vec{k}_m^-) - I(\vec{k}_m^+, \vec{k}_s^-)] \\ &= -\langle \psi_s^- | J_z | \psi_m^+ \rangle_{av}^*,\end{aligned}\quad (5)$$

with

$$I(\vec{k}_a^\pm, \vec{k}_b^\pm) = (N/2m) \int_0^d d^3r \psi_a^{\pm*} p_z \psi_b^\pm.$$

Again using the symmetry described above, we find that $I(\vec{k}_a^-, \vec{k}_b^-) = -I^*(\vec{k}_a^+, \vec{k}_b^+)$ and $I(\vec{k}_a^-, \vec{k}_b^-) = -I^*(\vec{k}_a^+, \vec{k}_b^+)$. It is convenient to absorb the phase factors into the coefficients by defining, for example, $\alpha' = \alpha e^{ik_{z,s}d}$, etc. The matching conditions for $z=d$ now can be recast as

$$\begin{aligned}\alpha' \hbar k_{z,s} / m^* &= \gamma' [I(\vec{k}_s^+, \vec{k}_m^+) - I(\vec{k}_m^-, \vec{k}_s^-)] + \delta' [I(\vec{k}_s^+, \vec{k}_m^-) \\ &\quad - I(\vec{k}_m^+, \vec{k}_s^-)], \\ \beta' \hbar k_{z,s} / m^* &= \gamma' [I(\vec{k}_s^+, \vec{k}_m^-) - I(\vec{k}_m^+, \vec{k}_s^-)]^* + \delta' [I(\vec{k}_s^+, \vec{k}_m^+) \\ &\quad - I(\vec{k}_m^-, \vec{k}_s^-)]^*.\end{aligned}\quad (6)$$

Restricting ourselves to cases in which only states with small $k_{z,s}$ are involved, i.e., states that are close to the bottom of the conduction band in the semiconductor, we may expand the integrals to first order in $k_{z,s}$ as

$$\begin{aligned}I(\vec{k}_s^+, \vec{k}_m^+) - I(\vec{k}_m^-, \vec{k}_s^-) &= \Xi_0(\vec{k}_m^+) + k_{z,s} \Xi_1(\vec{k}_m^+), \\ I(\vec{k}_s^+, \vec{k}_m^-) - I(\vec{k}_m^+, \vec{k}_s^-) &= -\Xi_0^*(\vec{k}_m^+) + k_{z,s} \Xi_1^*(\vec{k}_m^+).\end{aligned}\quad (7)$$

We may then write the interface matching conditions in compact form as

$$\begin{aligned}\alpha' (\hbar k_{z,s} / m^*) &= \gamma' (\Xi_0 + k_{z,s} \Xi_1) + \delta' (-\Xi_0^* + k_{z,s} \Xi_1^*), \\ \beta' (\hbar k_{z,s} / m^*) &= \gamma' (-\Xi_0 + k_{z,s} \Xi_1) + \delta' (\Xi_0^* + k_{z,s} \Xi_1^*).\end{aligned}\quad (8)$$

Rearranging these equations, assuming incidence from the semiconductor ($\delta' = 0$), and renaming $\gamma' = T$ we obtain

$$\mathbf{T} = \frac{4k_{z,s}^0 \text{Re}(\chi)}{[\Phi_1^2 + (k_{z,s}^0 \lambda)^2 \Phi_2^2] |\chi|^2 + [\Phi_1'^2 + (k_{z,s}^0 \lambda)^2 \Phi_2'^2] + 2k_{z,s}^0 \text{Re}(\chi) + 2[\Phi_1' \Phi_1 + (k_{z,s}^0 \lambda)^2 \Phi_2' \Phi_2] \text{Im}(\chi)}.\quad (14)$$

For a given metal/semiconductor interface χ is a function of $k_{z,m}$, but it does not depend on the potential barrier in region II. The requirement that the total electron energy E , in addition to the wave vector \vec{k}_\parallel , be conserved implies a relation-

$$\begin{aligned}\alpha' + \beta' &= (2m^*/\hbar) T \Xi_1, \\ (\alpha' - \beta') k_{z,z} &= (2m^*/\hbar) T \Xi_0.\end{aligned}\quad (9)$$

Noting that the right-hand sides of these equations are independent of $k_{z,s}$, it is straightforward to insert the results for α and β found above,

$$\begin{aligned}\sum_{k_{z,s} \geq 0} \{ [(1+R)\hat{\Phi}_1(k_{z,s}) + ik_{z,s}^0 \lambda (1-R)\hat{\Phi}_2(k_{z,s})] e^{ik_{z,s}d} \\ + [(1+R)\hat{\Phi}_1(-k_{z,s}) + ik_{z,s}^0 \lambda (1-R)\hat{\Phi}_2(-k_{z,s})] e^{-ik_{z,s}d} \} \\ = (2m^*/\hbar) T \Xi_1, \\ \sum_{k_{z,s} \geq 0} \{ [(1+R)k_{z,s} \hat{\Phi}_1(k_{z,s}) \\ + ik_{z,s}^0 \lambda (1-R)k_{z,s} \hat{\Phi}_2(k_{z,s})] e^{ik_{z,s}d} - [(1+R)k_{z,s} \hat{\Phi}_1(-k_{z,s}) \\ + ik_{z,s}^0 \lambda (1-R)k_{z,s} \hat{\Phi}_2(-k_{z,s})] e^{-ik_{z,s}d} \} = (2m^*/\hbar) T \Xi_0.\end{aligned}\quad (10)$$

Inverting the Fourier transformation, we obtain

$$\begin{aligned}(1+R)\Phi_1(d) + ik_{z,s}^0 \lambda (1-R)\Phi_2(d) &= (2m^*/\hbar) T \Xi_1 \\ -i(1+R)\Phi_1'(d) + k_{z,s}^0 \lambda (1-R)\Phi_2'(d) &= (2m^*/\hbar) T \Xi_0.\end{aligned}\quad (11)$$

Solving these equations for R and T and using that the Wronskian of Φ_1 and Φ_2 is constant yield

$$\begin{aligned}R &= \frac{i(\Xi_0/\Xi_1)(\Phi_1 + ik_{z,s}^0 \lambda \Phi_2) - (\Phi_1' + ik_{z,s}^0 \lambda \Phi_2')}{i(\Xi_0/\Xi_1)(\Phi_1 - ik_{z,s}^0 \lambda \Phi_2) - (\Phi_1' - ik_{z,s}^0 \lambda \Phi_2')}, \\ T &= \frac{-\hbar k_{z,s}^0}{m^* [(\Phi_1 - ik_{z,s}^0 \lambda \Phi_2) \Xi_0 + i(\Phi_1' - ik_{z,s}^0 \lambda \Phi_2') \Xi_1]},\end{aligned}\quad (12)$$

where the envelope functions and their derivatives are evaluated at $z=d$.

Finally, introducing the electron velocity in the relevant metal state as v_m , we obtain the transmission coefficient: $\mathbf{T} = [v_m / (\hbar k_{z,s}^0 / m^*)] |T|^2$. Exploiting reciprocity in the form $(\hbar k_{z,s}^0 / m^*) v_m = 4k_{z,s} \text{Re}(\Xi_0 \Xi_1^*)$ and defining $\chi = \Xi_0 / \Xi_1$ yield

ship between $k_{z,s}^0$ and $k_{z,m}$: $E = E_s(\vec{k}_\parallel, k_{z,s}) = E_m(\vec{k}_\parallel, k_{z,m})$, where E_s and E_m are the relevant bands in the semiconductor and the metal, respectively. Hence, the transmission coefficient may be expressed as a function of \vec{k}_\parallel and E , and the current

density is then calculated as an integral of the form

$$J(V) = -\frac{e}{\hbar} 2 \left(\frac{1}{2\pi} \right)^3 \int dE d^2 k_{\parallel} \mathbf{T}(\vec{k}_{\parallel}, E, V) [f(E) - f(E + eV)], \quad (15)$$

where $f(E)$ is the Fermi function and V is the voltage dropped across the potential barrier and the semiconductor/metal junction. The relationship of the transmission coefficient to the shape of the barrier and thus to the applied voltage across the semiconductor/metal contact is contained in the wave functions Φ_1 and Φ_2 and their derivatives at the interface.

Turning now to the case of a ferromagnetic metal, we find that the spin dependence of the transmission coefficient enters through the difference in $k_{z,m}$ for spin-up and spin-down electrons near the Fermi energy. Consequently, the parameter χ depends on the spin and may be written as $\chi_{\uparrow}, \chi_{\downarrow}$. The tunneling current is then spin polarized, and the charge- and spin-current densities may be calculated in analogy to the above relationship as

$$J(V) = -\frac{e}{\hbar} \left(\frac{1}{2\pi} \right)^3 \int dE d^2 k_{\parallel} [\mathbf{T}_{\uparrow}(\vec{k}_{\parallel}, E, V) + \mathbf{T}_{\downarrow}(\vec{k}_{\parallel}, E, V)] [f(E) - f(E + eV)], \quad (16)$$

$$J_s(V) = -\frac{e}{\hbar} \left(\frac{1}{2\pi} \right)^3 \int dE d^2 k_{\parallel} [\mathbf{T}_{\uparrow}(\vec{k}_{\parallel}, E, V) + \mathbf{T}_{\downarrow}(\vec{k}_{\parallel}, E, V)] [f(E) - f(E + eV)]. \quad (17)$$

The result for the transmission coefficient [Eq. (14)] forms the basis of our numerical calculations described in Sec. III. However, useful insight is gained by considering the simpler approximate expression for the transmission coefficient that is obtained by expanding Eq. (14) to lowest (linear) order in $k_{z,s}^0$,

$$\mathbf{T} = \frac{4k_{z,s}^0 \text{Re}(\chi)}{\Phi_1^2 [|\chi|^2 + (\Phi_1'/\Phi_1)^2 + 2(\Phi_1'/\Phi_1)\text{Im}(\chi)]}. \quad (18)$$

Clearly, the transmission coefficient depends on χ and Φ_1'/Φ_1 , with only the latter being voltage dependent. The spin-transmission coefficient, $\mathbf{T}_{\uparrow} - \mathbf{T}_{\downarrow}$, in this approximation becomes

$$\mathbf{T}_{\uparrow} - \mathbf{T}_{\downarrow} \approx 4k_{z,s}^0 \frac{(\chi_{\uparrow} - \chi_{\downarrow}) [(\ln \Phi_1)'^2 - \chi_{\uparrow} \chi_{\downarrow}]}{\Phi_1^2 [\chi_{\uparrow}^2 \chi_{\downarrow}^2 + (\chi_{\uparrow}^2 + \chi_{\downarrow}^2) (\ln \Phi_1)'^2 + (\ln \Phi_1)'^4]}. \quad (19)$$

Here we took $\chi_{\uparrow, \downarrow}$ to be real, consistent with the estimates discussed below. The term $[(\ln \Phi_1)'^2 - \chi_{\uparrow} \chi_{\downarrow}]$ in the numerator in Eq. (19) clearly shows that the voltage dependence of the logarithmic derivative of Φ_1 may control the sign of the spin transmission.

III. RESULTS

Considering specific examples requires an estimate of the interface coupling parameters χ for majority and minority

spins in the ferromagnetic metal. In general χ may be complex. For free particles one obtains the very simple (real) result: $\chi = k_{z,m}$. Generalization of this result to interfaces between different materials has been discussed within the context of effective-mass theory. One frequently used formulation gives¹⁵

$$\chi = k_{z,m} (m^*/m_m^*)^{-\beta}. \quad (20)$$

Here, m_m^* denotes the effective mass of the electrons in the metal near the Fermi energy and m^* is the effective mass in the semiconductor. The exponent, β , can take on values in the range $-1 \leq \beta \leq 0$. For $m^* < m_m^*$ the coupling parameter χ increases with increasing β .

We use this approximation for χ in the numerical results described below. To minimize the number of free parameters we assume that majority and minority electrons in the ferromagnetic metal near the Fermi level have the same effective mass, which we take to be equal to the free-electron mass. In this model the values of $\chi_{\uparrow, \downarrow}$ are different for spin-up and spin-down electrons near the Fermi level because their wave vectors are different.

Finally, we need to specify the potential barrier in the semiconductor (region II) and determine the envelope functions $\Phi_1(z)$ and $\Phi_2(z)$. We specifically consider a parabolic space-charge potential of form $V(z) = 2\pi e^2 n_D z^2 / \kappa$, where n_D is the (ionized) donor density and κ is the semiconductor dielectric constant. In this case, $\Phi_1(z)$ and $\Phi_2(z)$ are parabolic cylinder functions, which may be written in terms of confluent hypergeometric functions.

For the case of small $k_{z,s}^0$, the transmission coefficient [Eq. (19)] may be evaluated analytically in the asymptotic limit of a thick barrier, i.e., large built-in potential, V_{bi} . In this asymptotic limit, $(\ln \Phi_1)'^2 = d^2 / \lambda_p^4$, with $1/\lambda_p^4 = 4\pi e^2 n_D m^* / \hbar^2 \kappa$ and $d^2 = (V_{bi} - V) \kappa / (2\pi e n_D)$. In that case $\mathbf{T}_{\uparrow} - \mathbf{T}_{\downarrow}$ [Eq. (19)] changes sign for an applied voltage V that satisfies

$$e(V_{bi} - V) = \frac{\hbar^2 k_{F\uparrow} k_{F\downarrow}}{2m} \left(\frac{m^*}{m} \right)^{2\beta-1} = \sqrt{E_{F\uparrow} E_{F\downarrow}} \left(\frac{m^*}{m} \right)^{2\beta-1}. \quad (21)$$

Numerical results

Returning now to the more general expression of Eq. (14) for the transmission coefficient, we calculate the spin and charge current densities and their ratio, the current polarization, numerically. Although our model is quite general, in order to be specific, we now focus on the system consisting of Fe as the ferromagnetic metal and GaAs as the semiconductor. We use¹⁶ $k_{F\uparrow} = 1.09A^{-1}$ and $k_{F\downarrow} = 0.416A^{-1}$, $m^* = 0.067m$,¹⁷ and a Schottky barrier height (Φ_B) of 0.7 eV.¹⁸ This is the value used for Φ_B unless explicitly stated otherwise.

The structures investigated experimentally usually have nonuniform doping: a layer immediately adjacent to the metal is heavily doped and the bulk of the semiconductor is lightly doped. We approximate this situation by allowing for a high (ionized) donor density ($n_D = 5 \times 10^{18} \text{ cm}^{-3}$, unless ex-

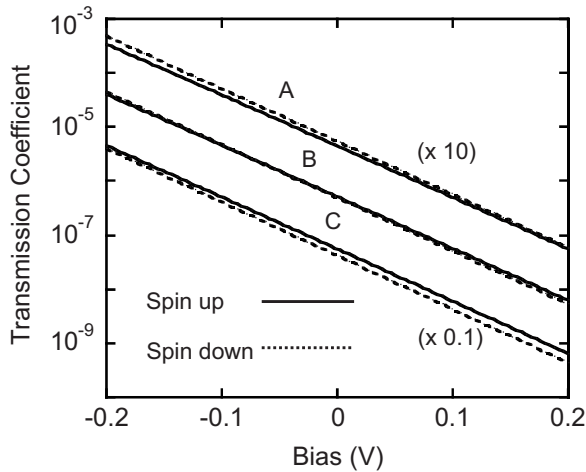


FIG. 2. Calculated transmission coefficients for spin-up and spin-down electrons with energy corresponding to the Fermi level in the semiconductor (GaAs) and $k_{\parallel}=0$ as a function of applied voltage. Results are shown for three different values of the interface coupling parameter β : (A) $\beta=-0.6$, (B) $\beta=-0.7$, and (C) $\beta=-0.8$. The results of A are enlarged by a factor of 10 and those of C are reduced by a factor of 0.1 to allow the curves to be clearly distinguishable.

explicitly stated otherwise) when calculating the space-charge induced potential profile but using a low electron concentration ($n=5 \times 10^{16} \text{ cm}^{-3}$) when we set the bulk ($T=0 \text{ K}$) semiconductor Fermi energy that determines the range of integration in the calculation of the currents [Eqs. (16) and (17)].

Figure 2 shows the calculated transmission coefficients for both spin orientations at an energy corresponding to the Fermi level in the semiconductor and $k_{\parallel}=0$ as a function of applied voltage. Positive voltage corresponds to a reverse biased Schottky contact, i.e., injection of electrons from the metal into the semiconductor. The transmission coefficient decreases monotonically with increasing bias; however, the much greater supply of electrons to be transmitted under reverse bias ensures that the current increases with increasing voltage. Results are shown on semilogarithmic scale for several different values of β and shifted by factors of 10 ($\beta=-0.6$) and 0.1 ($\beta=-0.8$) for clarity. Evidently, the calculated results for spin-up and spin-down transmission coefficients can cross at relatively small applied bias for certain coupling strengths. The reversal in sign of the difference in transmission coefficients is seen more clearly in Fig. 3, which shows the results of Fig. 2 plotted as $2(\mathbf{T}_{\uparrow}-\mathbf{T}_{\downarrow})/(\mathbf{T}_{\uparrow}+\mathbf{T}_{\downarrow})$ on a linear scale.

Figure 4 shows results for the spin polarization of the current, J_s/J , as a function of the applied voltage for a range of different β values. It is readily seen that the integrations involved in calculating the current from the energy- and k_{\parallel} -dependent transmission coefficients do not eliminate the change in sign of spin polarization, which may occur at relatively small positive or negative applied bias.

Evidently, the bias dependence of the spin polarization of the current does not only depend on the coupling across the metal semiconductor interface, here expressed through the exponent β . As pointed out above, the voltage dependence of the tunnel barrier plays a crucial role. Hence, the effect is

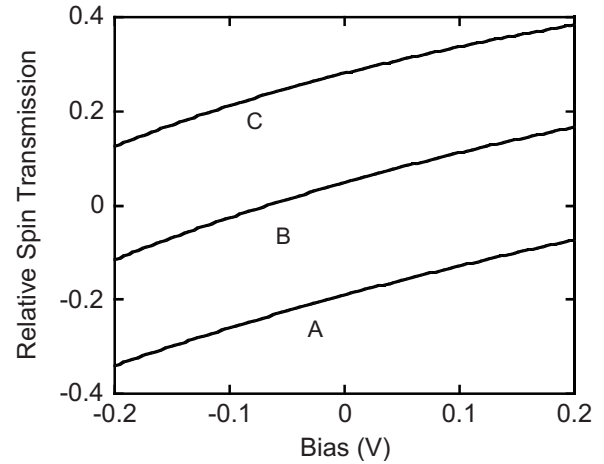


FIG. 3. Results of Fig. 2 shown as the normalized relative spin-transmission coefficient, $2(\mathbf{T}_{\uparrow}-\mathbf{T}_{\downarrow})/(\mathbf{T}_{\uparrow}+\mathbf{T}_{\downarrow})$, for electrons with energy corresponding to the Fermi level in the semiconductor and $k_{\parallel}=0$ as a function of applied voltage.

also strongly dependent on the height of the equilibrium Schottky barrier and on the doping level in the semiconductor just beneath the interface. The former dependence is explored in Fig. 5 for a range of Schottky barrier heights and fixed values of β and n_D . Figure 6 shows the complementary results for several different doping concentrations and fixed β and Schottky barrier values.

IV. CONCLUSIONS

A treatment of the transmission through a semiconductor tunnel barrier at a semiconductor/ferromagnetic metal contact shows that the spin-current polarization of the injected

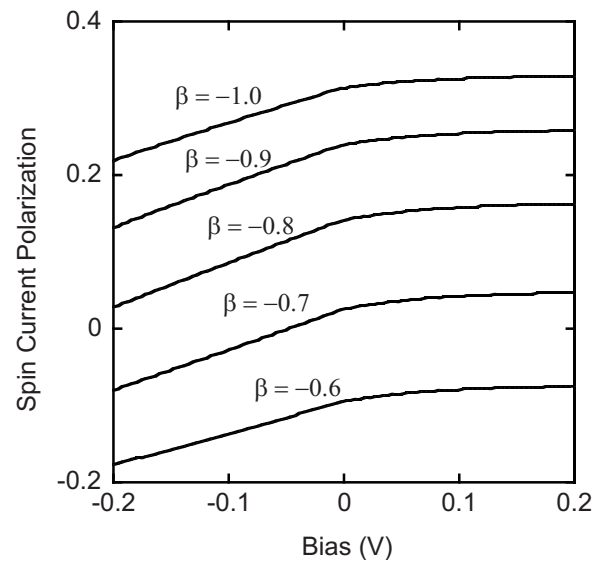


FIG. 4. Calculated current spin polarization as a function of applied bias across a GaAs/Fe Schottky contact with several different values for the parameter β . The barrier height is taken as $\Phi_B=0.7 \text{ eV}$ and the doping density near the metal/semiconductor interface as $n_D=5 \times 10^{18} \text{ cm}^{-3}$ in all cases.

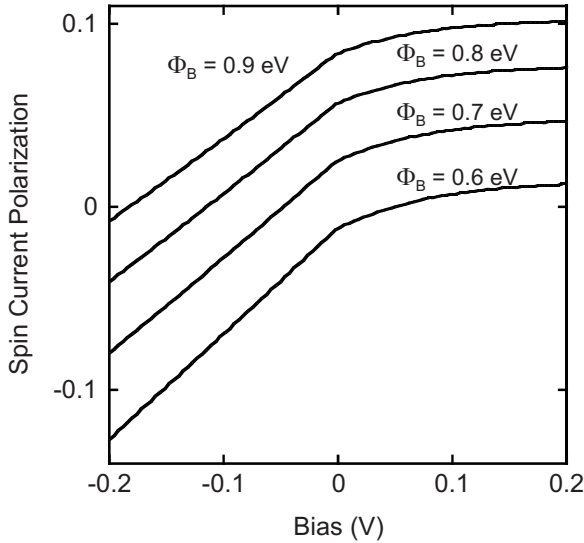


FIG. 5. Calculated current spin polarization as a function of applied bias across a GaAs/Fe Schottky contact for several different values of the barrier height. The parameter β is taken as $\beta = -0.7$ and the doping density near the metal/semiconductor interface as $n_D = 5 \times 10^{18} \text{ cm}^{-3}$ in all cases.

(or extracted) electrons can depend quite strongly on the bias across the junction and may even change sign as a function of bias. This phenomenon can arise from the voltage induced change in the shape of the potential barrier, which affects the transmission coefficients for the two spin orientations to different degrees. The discussion of the numerical results here focused on a parabolic potential barrier; however this restriction is not essential and the basic approach is readily generalized as shown in the Appendix.

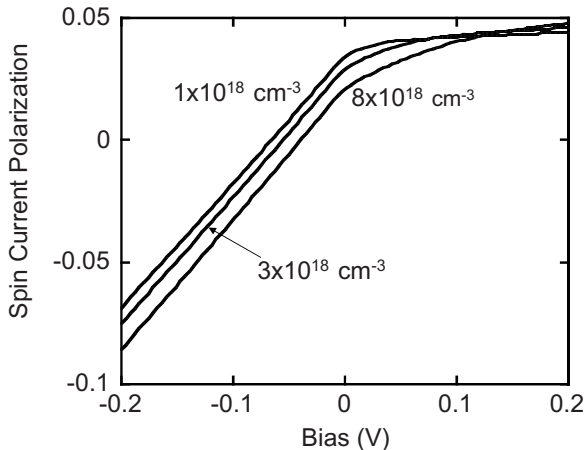


FIG. 6. Calculated current spin polarization as a function of applied bias across a GaAs/Fe Schottky contact for several different values of the doping concentration near the metal/semiconductor interface. The parameter β is taken as $\beta = -0.7$ and the Schottky barrier height as $\Phi_B = 0.7 \text{ eV}$ in all cases.

The principal parameter that controls the voltage dependence of interest is the effective coupling coefficient χ . A predictive determination of this quantity is not within the scope of the bulk electronic structures that form the basis of our model. It is precisely at this point that the mesoscale model discussed here links with the microscopic calculation of Chantis *et al.*¹¹ The latter stresses the physics of the microscopic interface but disregards the effects occurring over the greater length scale of the depletion region. On the other hand, it may, in fact, be argued that an effective coupling constant across the interface could depend sensitively on details of the contact fabrication, which are not entirely controlled. Hence, different χ values may be appropriate for different samples and that this may account for the observation that changes in sign of the current polarization are observed at positive applied bias in some cases but negative applied bias in others.⁹

An additional spin dependent mechanism in GaAs/Fe Schottky contacts arises from the (relatively weak) spin-orbit interaction. This effect is not considered in the present work, but it was recently argued that it may play a role in the measured anisotropic magnetoresistance of these devices.¹⁹ It is of course also possible that, for specific material systems, details of the electronic structure at the interface contribute to the voltage dependence of the spin current, for example, if the local interface densities of states for the two spin directions vary rapidly near the Fermi level.

ACKNOWLEDGMENTS

P.P.R. gratefully acknowledges the hospitality of the Theoretical Division at Los Alamos National Laboratory (LANL). The work at LANL was supported in part by the DOE, Office of Basic Energy Sciences, Work Proposal No. 08SCPE973.

APPENDIX

The effective-mass treatment outlined above can be discretized and solved numerically for arbitrary potential shape by adopting a formalism based on tight-binding electronic structure calculations. Discretizing the z axis in small increments a (a quasilattice constant, although in practice chosen to be much smaller than the real crystal lattice constant) and writing the bulk transfer-matrix elements as $t_s = \hbar^2 / (2m^*a^2)$ and $t_m = \hbar^2 / (2ma^2)$, one can readily generate the bulk bands of the semiconductor and the metal in effective-mass approximation provided that t_s and t_m are sufficiently large, i.e., a is chosen to be sufficiently small. The voltage dependent potential appears as part of the local site energies, and the transmission through that barrier is easily calculated following the iterative method outlined in Ref. 20. An advantage of this approach is that complex doping profiles are readily incorporated. The semiconductor/metal interface matching condition then reduces to choosing the (in general complex) transfer-matrix element across the interface. The connection between that parameter and the usual effective-mass interface matching conditions has been previously explored.²¹

- ¹I. Zutic, J. Fabian, and S. Das Sarma, *Rev. Mod. Phys.* **76**, 323 (2004).
- ²G. Schmidt, D. Ferrand, L. W. Molenkamp, A. T. Filip, and B. J. van Wees, *Phys. Rev. B* **62**, R4790 (2000).
- ³E. I. Rashba, *Phys. Rev. B* **62**, R16267 (2000); D. L. Smith and R. N. Silver, *Phys. Rev. B* **64**, 045323 (2001).
- ⁴J. H. Zhu, M. Ramsteiner, H. Kostial, M. Wassermeier, H.-P. Schonherr, and K. H. Ploog, *Phys. Rev. Lett.* **87**, 016601 (2001).
- ⁵A. T. Hanbicki, O. M. J. van't Erve, R. Magno, G. Kioseoglou, C. H. Li, B. T. Jonker, G. Itskos, R. Mallory, M. Yasar, and A. Petrou, *Appl. Phys. Lett.* **82**, 4092 (2003).
- ⁶B. T. Jonker, G. Kioseoglou, A. T. Hanbicki, C. H. Li, and P. E. Thompson, *Nat. Phys.* **3**, 542 (2007).
- ⁷S. O. Valenzuela, D. J. Monsma, C. M. Markus, V. Narayana-murti, and M. Tinkham, *Phys. Rev. Lett.* **94**, 196601 (2005).
- ⁸S. A. Crooker, M. Furis, X. Lou, C. Adelman, D. L. Smith, C. J. Palmstrom, and P. A. Crowell, *Science* **309**, 5744 (2005).
- ⁹X. Lou, C. Adelman, S. A. Crooker, E. S. Garlid, J. Zhang, K. S. M. Reddy, S. D. Flexner, C. J. Palmstrom, and P. A. Crowell, *Nat. Phys.* **3**, 197 (2007).
- ¹⁰J. Moser, M. Zenger, C. Gerl, D. Schuh, R. Meier, P. Chen, G. Bayreuther, W. Wegscheider, D. Weiss, C.-H. Lai, R.-T. Huang, M. Kosuth, and H. Ebert, *Appl. Phys. Lett.* **89**, 162106 (2006).
- ¹¹A. N. Chantis, K. D. Belashchenko, D. L. Smith, E. Y. Tsymbal, M. van Schilfgaarde, and R. C. Albers, *Phys. Rev. Lett.* **99**, 196603 (2007).
- ¹²H. Dery and L. J. Sham, *Phys. Rev. Lett.* **98**, 046602 (2007).
- ¹³Early results of this work were presented in P. P. Ruden and D. L. Smith, March Meeting of the American Physical Society, Denver, CO 2007 (unpublished), Paper No. BAPS.2007.MAR.B12.9. (<http://meetings.aps.org/link/BAPS.2007.MAR.B12.9>)
- ¹⁴J. Bardeen, *Phys. Rev. Lett.* **6**, 57 (1961).
- ¹⁵D. L. Smith and C. Mailhot, *Rev. Mod. Phys.* **62**, 173 (1990).
- ¹⁶M. B. Stearns, *J. Magn. Magn. Mater.* **5**, 167 (1977).
- ¹⁷*Numerical Data and Functional Relationships in Science and Technology*, Landolt-Bornstein New Series, Group III: Crystal and Solid State Physics, Vol. 22, edited by O. Madelung and M. Schulz (Springer-Verlag, Berlin, 1987).
- ¹⁸J. R. Waldrop, *Appl. Phys. Lett.* **44**, 1002 (1984).
- ¹⁹J. Moser, A. Matos-Abiague, D. Schuh, W. Wegscheider, J. Fabian, and D. Weiss, *Phys. Rev. Lett.* **99**, 056601 (2007).
- ²⁰W. A. Harrison, *Applied Quantum Mechanics* (World Scientific, Singapore, 2000).
- ²¹W. A. Harrison and A. Kozlov, in *Proceedings of the 21st International Conference on the Physics of Semiconductors*, edited by P. Jiang and H.-Z. Zheng (World Scientific, Singapore, 1993), Vol. 1, p. 341.